

Competition between Energy Transfer and Interligand Electron Transfer in Porphyrin–Osmium(II) Bis(2,2':6',2''-terpyridine) Dyads

Andrew C. Benniston, Anthony Harriman,* Consuelo Pariani, and Craig A. Sams

Molecular Photonics Laboratory, School of Natural Sciences, Bedson Building, University of Newcastle, Newcastle upon Tyne, NE1 7RU, United Kingdom

Received: May 5, 2007; In Final Form: July 3, 2007

Rapid intramolecular energy transfer occurs from a free-base porphyrin to an attached osmium(II) bis(2,2':6',2''-terpyridine) complex, most likely by way of the Förster dipole–dipole mechanism. The initially formed metal-to-ligand, charge-transfer (MLCT) excited-singlet state localized on the metal complex undergoes very fast intersystem crossing to form the corresponding triplet excited state ($^3\text{MLCT}$). This latter species transfers excitation energy to the $^3\pi,\pi^*$ triplet state associated with the porphyrin moiety, such that the overall effect is to catalyze intersystem crossing for the porphyrin. Interligand electron transfer (ILET) to the distal terpyridine ligand, for which there is no driving force, competes poorly with triplet energy transfer from the proximal $^3\text{MLCT}$ to the porphyrin. Equipping the distal ligand with an ethynylene residue provides the necessary driving force for ILET and this process now competes effectively with triplet energy transfer to the porphyrin. The rate constants for all the relevant processes have been derived from laser flash photolysis studies.

Introduction

The relatively long-lived, triplet excited states of Ru(II) and Os(II) poly(pyridine) complexes have found numerous applications as sensitizers, photocatalysts, luminescent sensors, and electron-transfer mediators. In the absence of highly conjugated substituents, the lowest energy triplet states of such materials are of metal-to-ligand, charge-transfer (MLCT) character and often display modest yields of luminescence at ambient temperature. After much debate, it is now reasonably well-established that, in a polar solvent, the MLCT triplet state has the electron density localized on a single poly(pyridine) ligand at any given moment. The promoted electron hops between the coordinated ligands in an incoherent manner and on a fast time scale.¹ Experimental measurement of the rate of interligand electron transfer (ILET) is rendered difficult by the absence of obvious spectroscopic signatures and the most convincing evidence has accrued from time-resolved polarization anisotropy studies.² Here, the dynamics of ILET occur with characteristic time constants of 47³ and 8.7⁴ ps, respectively, for Ru(II) and Os(II) tris(2,2'-bipyridine) complexes, where there is no thermodynamic driving force. In asymmetric complexes, the time scale for ILET increases and is notably faster for Os(II) than for Ru(II).⁴ A different approach for measuring the rate of ILET was introduced recently by Meyer and Papanikolis⁵ whereby this process was in competition with triplet-energy transfer (TET) to an appended anthracene residue. Related work by Hammarström et al.⁶ found that electron transfer from the excited state of a Ru(II) tris(2,2'-bipyridine) complex to a covalently attached methyl viologen residue occurred within 4 ps and this rate seems to be at odds with the idea of fairly slow ILET. Subsequent studies using ultrafast laser excitation and transient absorption anisotropy measurements indicated⁷ that the ILET process is complete within 1 ps. A problem with all experimental measurements reported to date, however, is that

excitation produces a statistical mixture of MLCT triplet states wherein the promoted electron resides on different ligands. The experiment then involves monitoring the approach to equilibrium. We now describe a different method by which to resolve ILET that overcomes this particular limitation.

The approach involves pulsed excitation of a porphyrin that is covalently attached to an Os(II) bis(2,2':6',2''-terpyridine) complex by way of a short spacer. The singlet excited state of the porphyrin ($^1\pi,\pi^*$) produced upon illumination transfers the excitation energy to the metal complex on a very fast time scale⁸ so as to generate the corresponding MLCT triplet state within a few picoseconds. The promoted electron resides solely on the proximal terpyridine (terpy) ligand. Because the porphyrin possesses a low-lying triplet excited state ($^3\pi,\pi^*$),⁸ intramolecular TET competes with ILET but energy transfer from the distal terpy ligand is relatively slow. This disparity in rates allows accurate screening of the ILET process and indeed all the various steps involved in the energy distribution network.

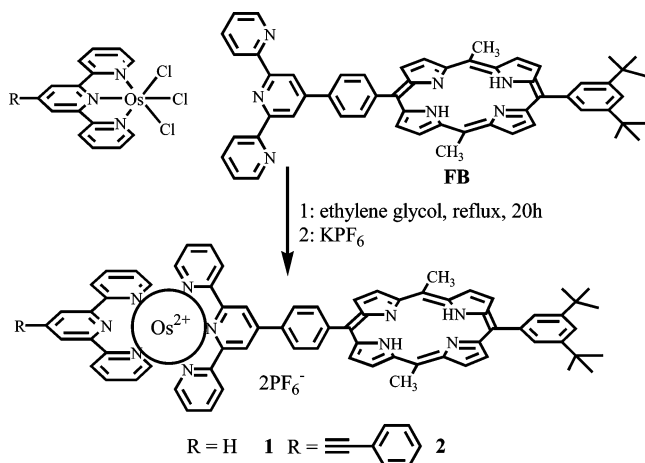
Experimental Section

The starting materials Os(terpy)Cl₃, Os(phterpy)Cl₃, and the free-base porphyrin precursor, **FB**, were prepared by literature methods.⁹ The new molecular dyads were prepared according to Scheme 1, with details given below. Samples were isolated as the hexafluorophosphate salts.

Preparation of 1. To a solution of Os(terpy)Cl₃ (32 mg, 0.06 mmol) in ethylene glycol (25 mL) was added **FB**⁷ (50 mg, 0.060 mmol). The solution was purged with dry N₂ for 15 min before being heated at reflux for 20 h. After cooling to room temperature, a saturated solution of aqueous KPF₆ was added until no additional precipitate formed. The dark solid was collected by filtration, washed with H₂O then Et₂O, and purified by silica gel column chromatography, using CH₃CN:H₂O:saturated KNO₃ (90:10:1) as eluant. The second band collected was reduced in volume and an aqueous KPF₆ solution was added to precipitate a black solid, which was filtered, washed with

* Address correspondence to this author. Phone/fax: 44-191-222-8660. E-mail: anthony.harriman@ncl.ac.uk.

SCHEME 1: Outlined Procedure Used To Prepare the Molecular Dyads Studied Herein and Their Molecular Formulas



H₂O then Et₂O, and dried. Yield 24 mg, 25%. An analytically pure sample of the compound was prepared by slow vapor diffusion of Et₂O into an acetonitrile solution of the complex. Analytical data for **1**: ¹H NMR (300 MHz, CD₃CN) δ (ppm) -2.62 (s, 2H, NH), 1.55 (s, 18H, C(CH₃)₃), 4.67 (s, 6H, CH₃), 7.13–7.19 (m, 2H), 7.29 (d, 2H, *J* = 6 Hz), 7.43 (d, 2H, *J* = 5 Hz), 7.80–7.86 (m, 4H), 7.94–7.96 (m, 2H), 8.10 (s, 2H), 8.51 (d, 2H, *J* = 8 Hz), 8.60–8.62 (m, 4H), 8.76–8.80 (m, 6H), 8.88 (d, 2H, *J* = 5 Hz), 9.01 (d, 2H, *J* = 5 Hz), 9.37 (s, 2H), 9.62–9.63 (d, 2H, *J* = 5 Hz), 9.68–9.69 (d, 2H, *J* = 5 Hz). MS (MALDI) *m/z* calcd for C₇₂H₆₂N₁₀OsPF₆ 1403.4, found 1403.4 (M - PF₆)⁺. Elemental analysis calcd (found) for C₇₂H₆₂N₁₀OsP₂F₁₂·7H₂O: C, 51.67 (51.59); H, 4.58 (3.83), 8.37 (7.98).

Preparation of 2. To a solution of Os(phterpy)Cl₃ (12 mg, 0.018 mmol) in butanol (25 mL) was added **FB**⁷ (15 mg, 0.018 mmol). The solution was purged with dried N₂ for 15 min before being heated at reflux for 20 h. After removing the solvent, CH₃CN was added and the compound was precipitated by addition of a saturated aqueous solution of KPF₆ until no additional solid deposited. The dark residue was collected by filtration, washed with H₂O then Et₂O, and purified by silica gel column chromatography, using CH₃CN:H₂O:saturated KNO₃ (98:2:1) as eluant. The second band collected was reduced in volume and an aqueous KPF₆ solution was added to precipitate a black solid, which was filtered, washed with H₂O and Et₂O, and then dried. Yield 5 mg, 17%. An analytically pure sample of the compound was prepared by slow vapor diffusion of Et₂O into an acetonitrile solution of the complex. Analytical data for **2**: ¹H NMR (300 MHz, CD₃CN) δ -2.62 (s, 2H, NH), 1.49 (s, 18H, C(CH₃)₃), 4.61 (s, 6H, CH₃), 7.06–7.20 (m, 4H), 7.25–7.40 (m, 4H), 7.45–7.56 (m, 4H), 7.63–7.88 (m, 8H), 8.04 (d, 2H, *J* = 1.8 Hz), 8.50–8.56 (m, 4H), 8.72 (d, 2H, *J* = 8 Hz), 8.82 (d, 2H, *J* = 5 Hz), 8.91 (s, 2H), 8.95 (d, 2H, *J* = 5 Hz), 9.32 (s, 2H), 9.56 (d, 2H, *J* = 5 Hz), 9.63 (d, 2H, *J* = 5 Hz). MS (MALDI) *m/z* calcd for C₈₀H₆₆N₁₀OsPF₆ 1502.7, found 1503.5 (M - PF₆)⁺.

Methods. Absorption spectra were recorded with a Hitachi U3310 spectrophotometer and emission spectra were recorded with a Jobin-Yvon Fluorolog tau-3 spectrophotometer. Optically dilute solutions were used for all spectroscopic studies, after thorough purging with dried N₂. Solvents used for spectroscopic studies were of the highest available commercial grade and were redistilled from appropriate drying agents prior to use. Fresh solutions were made for each experiment. An Applied Photo-

physics LKS.60 laser flash spectrometer was used for nano-second studies. The output from a frequency-doubled or frequency-tripled Nd:YAG laser (fwhm = 4 ns) was used to pump an OPO so as to obtain the required excitation wavelength. A pulsed Xe arc lamp was used for the monitoring beam and was directed through the sample cell at 90° to the excitation pulse. After passage through a high-radiance monochromator, the signal was detected with a PMT and sent to a PC for storage and subsequent data analysis. Triplet lifetimes were measured at a variety of monitoring wavelengths, for different excitation wavelengths, and signal averaged.

Improved time resolution was achieved with a mode-locked, frequency-doubled Nd:YAG laser (fwhm = 20 ps). The excitation pulse was passed through a Raman shifter to isolate the required wavelength. The monitoring pulse was either a white light continuum, delayed with respect to the excitation pulse with a computer-controlled optical delay line, or a pulsed Xe arc lamp. For the former studies, the two pulses were directed almost collinearly through the sample cell. The monitoring pulse was dispersed with a Spex spectrograph and detected with a dual-diode array spectrometer. Approximately 150 individual laser shots were averaged at each delay time.

Fast transient spectroscopy was made by pump-probe techniques, using femtosecond pulses delivered from a Ti:sapphire generator amplified with a multipass amplifier pumped via the second harmonic of a Q-switched Nd:YAG laser. The amplified pulse energies varied from 0.3 to 0.5 mJ and the repetition rate was kept at 10 Hz. Part of the beam (ca. 20%) was focused onto a second harmonic generator to produce the excitation pulse. The residual output was directed onto a 4-mm sapphire plate so as to create a white light continuum for detection purposes. The continuum was collimated and split into two equal beams. The first beam was used as reference while the second beam was combined with the excitation pulse and used as the diagnostic beam. The two beams were directed to different parts of the entrance slit of a cooled CCD detector and used to calculate differential absorbance values. The CCD shutter was kept open for 1 s and the accumulated spectra were averaged. This procedure was repeated until about 100 individual spectra had been averaged. Time-resolved spectra were recorded with a delay line stepped in increments of 100 fs for short time measurements. This step length was increased for longer time measurements. The decay profiles were fitted globally as the sum of exponentials and deconvoluted with a Gaussian excitation pulse. The group velocity dispersion across one spectrum (ca. 220 nm) was of the order of 1 ps and the overall temporal resolution of this setup was ca. 0.3 ps.

Results and Discussion

To explore the energy redistribution processes following selective excitation of such dyads, compounds **1** and **2** were synthesized by a modular approach (Scheme 1) and purified by extensive column chromatography. The reactants are linked through a connecting phenylene ring held almost orthogonal to the porphyrin nucleus. The acetylene residue in **2** plays a pivotal role insofar as it renders the attached terpy ligand (from now on designated the distal terpy) somewhat easier to reduce¹⁰ than the parent terpy. This lowers the energy of the resultant MLCT triplet state and provides the impetus for ILET. It should be noted that according to the results of cyclic voltammetry studies made with **1** and **2**, light-induced electron transfer is unlikely to compete with the various energy-transfer steps. Thus, the most thermodynamically favorable process involves oxidation of the Os^{II} center by the singlet excited state localized on the

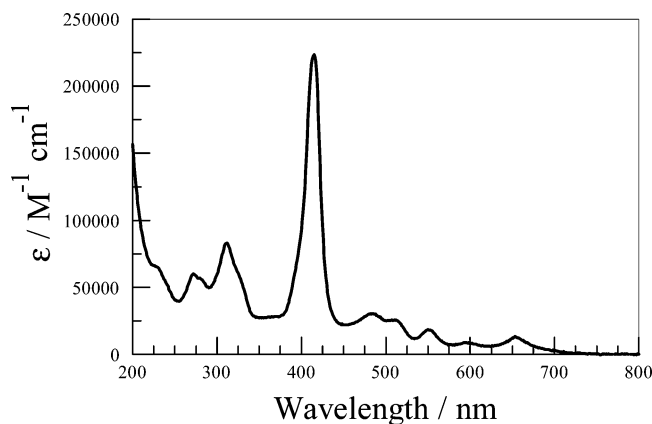


Figure 1. Absorption spectrum recorded for dyad **1** in acetonitrile solution. The MLCT transition associated with the Os^{II} complex appears at 485 nm and as a long tail stretching into the near-IR. The most prominent bands due to the porphyrin are at 420, 512, and 554 nm. The transitions seen between 270 and 350 nm are assigned to the Os^{II} complex.

porphyrin unit, for which $\Delta G^0 = -0.08$ eV in both cases. All other conceivable electron-transfer steps are strongly endergonic. There is a growing awareness that the second excited singlet state resident on the porphyrin can be used to drive electron-transfer reactions¹¹ but the S_2 state for the porphyrin unit used here is very short-lived¹² and unlikely to enter into secondary reactions.

There have been several reports of intramolecular energy transfer in porphyrin–Ru(II) poly(pyridine) molecular dyads and related structures.^{8,13} These processes include both singlet-to-triplet ($^1\pi,\pi^* \rightarrow ^3\text{MLCT}$) and triplet-to-triplet ($^3\text{MLCT} \rightarrow ^3\pi,\pi^*$) energy transfer, such that the porphyrin-based $^3\pi,\pi^*$ state is formed in quantitative yield. An advantage provided by the corresponding Os(II)-based dyad is that the increased oscillator strength in the far red region, this being due to the spin-forbidden MLCT absorption transition, facilitates Förster-type energy transfer to the metal complex (Figure 1). Thus, excitation of dyads **1** and **2** at 420 nm, where only the porphyrin absorbs (Figure 1), does not result in the characteristic porphyrin-based fluorescence seen for compounds lacking the Os(II) complex. The extent of fluorescence quenching in acetonitrile solution at 20 °C exceeds 10^4 -fold and the excited singlet state lifetime of the porphyrin unit is <30 ps, as estimated by time-resolved fluorescence spectroscopy, compared to 10 ns for the parent porphyrin. Under these conditions, energy transfer can occur from both the S_2 ($^1\pi,\pi^* \rightarrow ^1\text{MLCT}$) and S_1 ($^1\pi,\pi^* \rightarrow ^3\text{MLCT}$) states localized on the porphyrin; in the former case rapid intersystem crossing within the Os(II) complex forms the lowest energy $^3\text{MLCT}$ state, while in the latter case fast internal conversion precedes energy transfer. Even at 77 K, fluorescence from the porphyrin unit is difficult to resolve from the background signal.

Transient differential absorption spectra recorded for both dyads after excitation with 4-ns laser pulses delivered at 420, 590, or 660 nm are characteristic of the π,π^* triplet excited state localized on the porphyrin unit (Figure 2). In deoxygenated acetonitrile at room temperature, the porphyrin triplet decays by way of first-order kinetics with a lifetime of ca. 35 μs to reform the ground state. No other species are involved on these time scales. Excitation at 660 nm leads to direct population of the $^3\text{MLCT}$ state associated with the Os(II)-based unit but energy transfer must occur within the 4-ns pulse since the only species observed is the porphyrin-based π,π^* triplet state. As a consequence, no emission is observed from the Os(II)-based

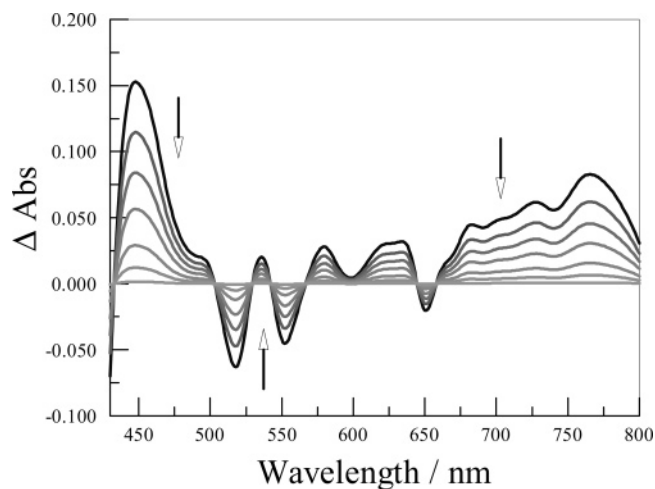


Figure 2. Transient differential absorption spectrum recorded after excitation of **1** in deoxygenated acetonitrile with a 4-ns laser pulse delivered at 480 nm. Individual spectra were recorded at different delay times within the window 100 ns to 50 μs .

unit in fluid solution, in contrast to the moderately strong luminescence seen around 700–800 nm for reference complexes lacking the porphyrin residue.¹⁴ On this basis, and taking due account of earlier work made with Ru(II)-based dyads,^{8,13} we can safely conclude that the $^3\text{MLCT}$ state transfers excitation energy to the appended porphyrin. There is a reasonable thermodynamic driving force for this process,¹⁵ which is expected to take place via the Dexter-type electron-exchange mechanism.^{8f,9} The overall reaction scheme, therefore, involves two successive energy-transfer steps; first from S_1 (or S_2) localized on the porphyrin to populate the $^3\text{MLCT}$ state and second TET to generate the $^3\pi,\pi^*$ localized on the porphyrin. Such behavior is fully consistent with earlier studies made with Ru^{II}-based dyads.^{8,13} The challenge for these new dyads, therefore, is to examine the role of the intermediate $^3\text{MLCT}$ state in relaying excitation energy between the porphyrin π,π^* excited states. Overall, this can be considered as a type of catalyzed intersystem crossing within the porphyrin manifold.

Laser flash photolysis studies with subpicosecond temporal resolution were carried out with dyad **1** in deoxygenated acetonitrile at room temperature. Following laser excitation at 420 nm, where the porphyrin unit is the sole chromophore, the characteristic transient absorption spectrum of the porphyrin excited singlet state is observed (Figure 3a). This species decays rapidly by way of first-order kinetics, with a globally averaged lifetime of 3.5 ± 0.4 ps. This latter value can be compared with the mean lifetime of 6 ps calculated for Förster-type, singlet–triplet energy transfer. Agreement is satisfactory, taking account of the uncertainties involved in both experiment and calculation, and is consistent with the total extinction of fluorescence from the porphyrin. Given that the same process is much slower in the corresponding Ru(II)-based analogues,⁸ where the mean lifetimes for population of the $^3\text{MLCT}$ state are around 2 ns, we conclude that the primary mechanism for intramolecular energy transfer involves dipole–dipole interactions. Because of the mutual orientation and separation distance, through-space energy transfer will preferentially populate the MLCT state(s) associated with the terpy ligand proximal to the porphyrin. The conclusion, therefore, is that selective excitation into the porphyrin unit leads to rapid formation of the proximal $^3\text{MLCT}$ state localized on the metal complex.

The transient absorption spectral records show the presence of the porphyrin $^3\pi,\pi^*$ state after decay of the S_1 state (Figure 3b). The porphyrin-based triplet state shows increased bleaching

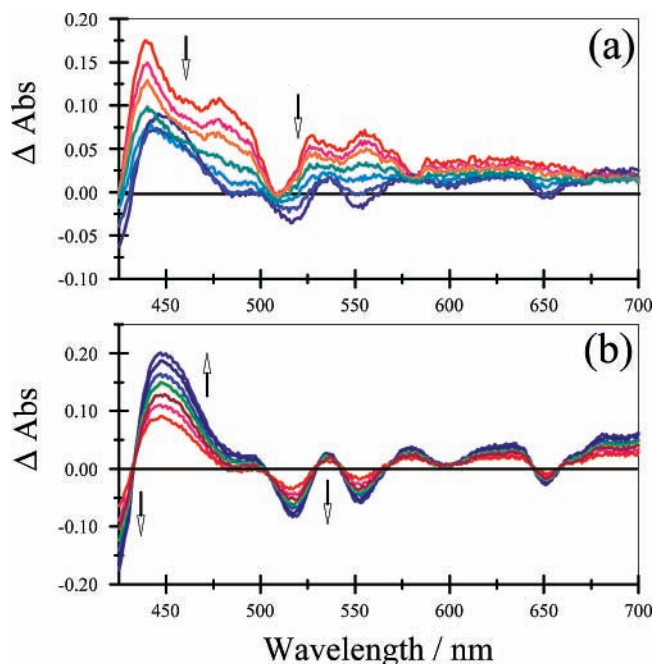


Figure 3. Transient differential absorption spectra recorded after subpicosecond laser excitation of **1** in deoxygenated acetonitrile at room temperature. (a) Spectra were recorded at delay times of 0, 0.8, 1.5, 3, 5, 8, and 12 ps and show the progressive loss of absorption due to the porphyrin-based S_1 state. (b) Spectra were recorded at delay times of 12, 16, 20, 25, 30, 40, and 50 ps and show the progressive gain of absorption due to the porphyrin-based T_1 state.

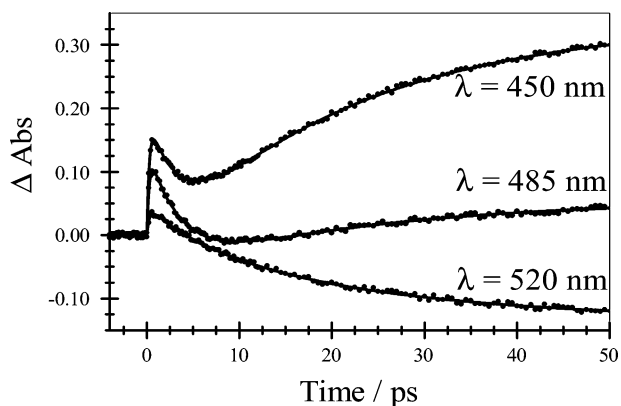


Figure 4. Decay traces obtained for the transient spectral records described in Figure 3. The solid lines represent the best nonlinear, least-squares fit to the model given as Scheme 2 and with the rate constants collected in Table 1.

at around 430 nm, strong absorption at 450 nm (slightly red-shifted from the S_1 absorption band), distinctive bleaching peaks at 520, 555, and 650 nm, and weak absorption in the far-red region. Kinetic traces recorded across the entire spectral range, however, show that there is a significant time lag between decay of S_1 and the appearance of T_1 (Figure 4). This becomes particularly evident on comparing kinetic traces recorded at 450 nm, where both S_1 and T_1 absorb strongly, at 485 nm, where S_1 absorbs more strongly than T_1 , and at 520 nm, where S_1 absorbs weakly but T_1 shows pronounced bleaching. Presumably, the time lag arises because of intermediate population of the ${}^3\text{MLCT}$ state but this is difficult to confirm by the spectral records. The transient absorption spectrum of the ${}^3\text{MLCT}$ was recorded for the corresponding Os^{II} complex lacking the porphyrin fragment and shows bleaching centered at 490 nm together with weak absorption at higher and lower energies.¹⁶ There are no obvious spectroscopic indicators in Figure 3 for

SCHEME 2: Overall Reaction Process Showing Rapid Formation of the Proximal ${}^3\text{MLCT}$ State, Followed by Competition between TET to the Porphyrin ${}^3\pi,\pi^*$ State and ILET

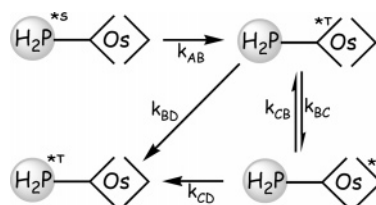


TABLE 1: Summary of the Kinetic Data Derived by Global Fitting of the Spectroscopic Data Obtained for Dyads 1 and 2 in Deoxygenated Acetonitrile at Room Temperature

rate constant (ps^{-1})	dyad 1	dyad 2
k_{AB}	0.24	0.29
k_{BD}	0.063	0.060
k_{BC}	0.031	0.100
k_{CB}^a	0.100	0.023
k_{CD}^b		0.018

^a Set by the appropriate equilibrium constant. ^b Not required for dyad 1.

transient formation of the ${}^3\text{MLCT}$ state and it is to be expected that this species will undergo fast TET to populate the porphyrin-based T_1 state. Analysis of the kinetic traces collected over the entire spectral window in terms of Scheme 2 allows computation of the relevant rate constants (Table 1) and confirms that the ${}^3\text{MLCT}$ state is relatively short-lived under these conditions. This scheme allows for ILET (k_{BC}) to compete with TET (k_{BD}), although this step is slightly endergonic ($\Delta E = 0.030$ eV). Assuming ILET is fully reversible, with the effective equilibrium constant ($K = 0.3$) being set by the energy gap, global analysis of the kinetic traces allows estimation of k_{BD} as being $6.3 \times 10^{10} \text{ s}^{-1}$. For dyad 1, the experimental kinetic traces could be reproduced by consideration of reversible ILET but without the need for direct TET from the distal ${}^3\text{MLCT}$ state to the ${}^3\pi,\pi^*$ state. That is to say, $k_{CD} < k_{CB}$, with the latter being set by the equilibrium conditions (Table 1); note well, the sole constraint imposed on this model is that the ratio k_{BC}/k_{CB} is set by the corresponding equilibrium constant. It is also important to stress that the only criterion for involvement of the ILET step is a better global fit to the experimental data—there is no direct spectroscopic evidence.

According to this analysis, TET from the proximal ${}^3\text{MLCT}$ state of **1** accounts for some 70% of the initial photonic energy, while ILET to the distal ${}^3\text{MLCT}$ state accounts for the remaining 30% (Figure 5a). The rate constant (k_{BD}) for TET from the proximal ${}^3\text{MLCT}$ state is comparable to values measured for related dyads.^{8,13} This step should fall within the Marcus inverted region since the energy gap ($\Delta E_{TT} = 0.33$ eV) greatly exceeds the total reorganization energy ($\lambda_{TT} = 0.10$ eV)¹⁷ for TET. Likewise, the rate constant (k_{BC}) for ILET from proximal to distal ${}^3\text{MLCT}$ states is similar to values measured for other Os^{II} poly(pyridine) complexes by polarization spectroscopy.⁴ In our scheme, the rate constant (k_{CB}) for ILET from distal to proximal ${}^3\text{MLCT}$ states is set by the equilibrium constant and again is in line with previous estimates.⁴ The ILET process has the overall effect of slowing the rate of TET to the ${}^3\pi,\pi^*$ state such that the growth of the latter species becomes nonexponential. However, the effect is small and energy transfer remains quantitative because of the fast time scales involved and the slow nonradiative decay of the various excited states.

Turning attention now to **2** it is notable that there is a small thermodynamic driving force ($\Delta E_{TT} = 0.042$ eV) for ILET from

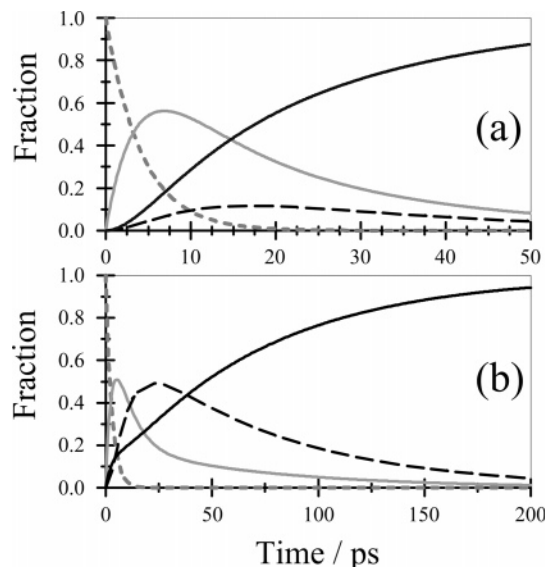


Figure 5. Projected population analysis for the S_1 (gray dashed), proximal $^3\text{MLCT}$ (long dashes), distal $^3\text{MLCT}$ (solid gray), and T_1 (solid black) states for (a) **1** and (b) **2**, according to Scheme 2 and using the rate constants collected in Table 1.

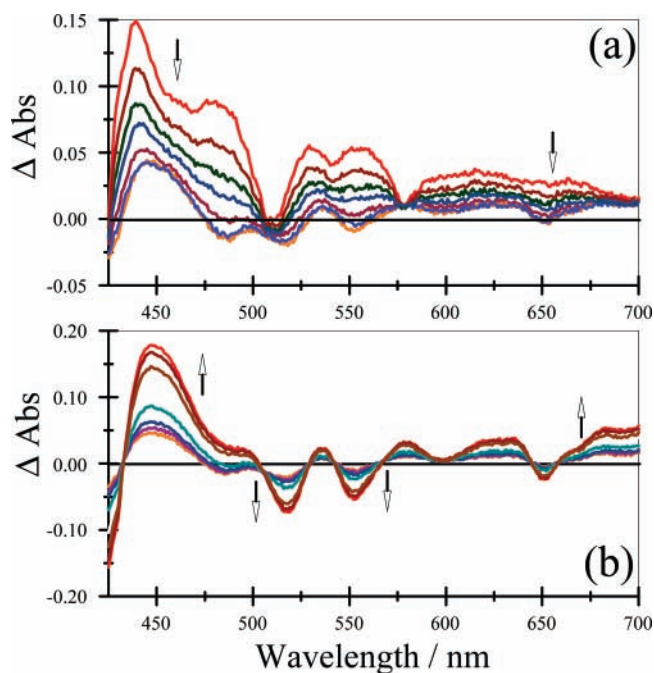


Figure 6. Transient differential absorption spectra recorded after subpicosecond laser excitation of **2** in deoxygenated acetonitrile at room temperature. (a) Spectra were recorded at delay times of 0, 1, 2, 3, 5, 8, and 12 ps and show the progressive replacement of absorption due to the porphyrin-based S_1 state by the $^3\text{MLCT}$ state. (b) Spectra were recorded at delay times of 15, 20, 25, 40, 70, 100, 150, and 200 ps and show the progressive gain of absorption due to the porphyrin-based T_1 state.

proximal to distal $^3\text{MLCT}$ states because of the effect of the ethyne substituent.¹⁸ The transient spectroscopic records again indicate that decay of the porphyrin S_1 state, which shows strong absorption at around 430 nm and pronounced bleaching signals at 515 and 580 nm, is extremely fast (Figure 6a). The rate constant, k_{AB} , derived from global analysis of the kinetic data is $2.9 \times 10^{11} \text{ s}^{-1}$ and this compares well with the rate constant ($k_{\text{F}} = 4 \times 10^{11} \text{ s}^{-1}$) calculated for Förster-type energy transfer. As for dyad **1**, it is assumed that energy transfer selectively populates the proximal $^3\text{MLCT}$ state localized on the metal

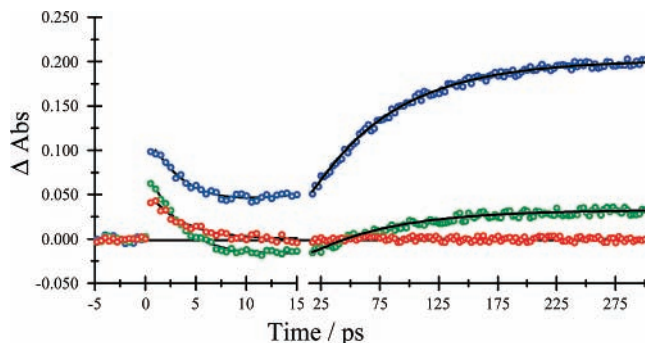


Figure 7. Kinetic traces recorded at 448 nm (blue), showing conversion of S_1 to T_1 , 485 nm (green), showing transient population of the $^3\text{MLCT}$ state, and at 529 nm (red), showing fast decay of the S_1 state.

complex. Close examination of the transient spectral records (Figure 6a) indicates that a weak bleach signal at around 485 nm develops over ca. 10 ps before being replaced by the characteristic differential absorption spectrum of the $^3\pi, \pi^*$ state. The negative signal at 485 nm can be attributed to transient population of the $^3\text{MLCT}$ state.¹⁶ Formation of the $^3\pi, \pi^*$ state, which possesses strong absorption at 440 nm and in the far-red region together with bleaching signals at 520, 555, and 650 nm, is remarkably slow compared to **1** (Figure 6b). Furthermore, global analysis indicates that formation of the porphyrin-based triplet state lags far behind decay of the S_1 state and does not correspond to a single-exponential process (Figure 7). Thus, clean decay of the S_1 state can be monitored at 529 nm where the other species show negligible absorption. Transformation of S_1 into T_1 can be followed at 448 nm, where the $^3\text{MLCT}$ state is essentially transparent and the porphyrin-based excited states absorb strongly. This decay trace shows clearly that decay of S_1 is very much faster than formation of T_1 . Finally, transient population of the $^3\text{MLCT}$ state is apparent from the definite bleaching signal seen at 485 nm. Recovery of a positive absorption signal takes many tens of picoseconds and is too slow to explain without invoking ILET.

A complete analysis was made in accordance to Scheme 2 and the rate constants derived from a global analysis are collected in Table 1. In this case, the spectral records provide clear evidence for intermediate population of the $^3\text{MLCT}$ state but without specifying which terpy ligand is involved. The delayed formation of the $^3\pi, \pi^*$ state, however, can be explained only in terms of competing ILET since the thermodynamics and geometry for TET from the proximal $^3\text{MLCT}$ to the $^3\pi, \pi^*$ remain exactly the same as for **1**. Global analysis of the kinetic data shows that energy transfer from the proximal $^3\text{MLCT}$ state to the $^3\pi, \pi^*$ state (k_{BD}) occurs at a rate comparable to that found for **1** under the same conditions but this step competes poorly with ILET to form the distal $^3\text{MLCT}$ state. The rate constant (k_{BC}) for this latter step is increased relative to **1** by a factor of ca. 6-fold, presumably due to the improved thermodynamics. Indeed, the equilibrium position ($K = 4.3$) now lies on the side of the distal $^3\text{MLCT}$ state. The rate constant (k_{CB}) for reverse population of the proximal $^3\text{MLCT}$ state is set by the equilibrium constant and is relatively small. The rate constant (k_{CD}) for TET from the distal $^3\text{MLCT}$ state is low, compared to TET from the proximal $^3\text{MLCT}$ state, because of the increased separation distance. We consider that this latter step occurs via long-range super-exchange interactions, for which the overall ΔE_{TT} is 0.33 eV.

The derived rate constants can be used to construct a population diagram for **2** (Figure 5b). As already noted for **1**, decay of the S_1 state is rapid and leads to transient formation

of the $^3\text{MLCT}$ state. On the assumption that intramolecular energy transfer preferentially populates the proximal $^3\text{MLCT}$ state, the transient records indicate fast build-up of this species. Decay of the proximal $^3\text{MLCT}$ state involves formation of both distal $^3\text{MLCT}$ and porphyrin-based $^3\pi,\pi^*$ states. Since ILET is competitive with TET, the distal $^3\text{MLCT}$ state accumulates over about 20 ps and reforms the proximal $^3\text{MLCT}$ state by reverse TET, thereby extending the lifetime of this latter species over some hundred picoseconds or so. The $^3\pi,\pi$ state continues to develop over about 200 ps and this can only be because of relatively fast ILET.

In seeking to confirm the ILET step we note that this process most likely occurs under adiabatic conditions,^{4,19} or at least close to the adiabatic–nonadiabatic interface.²⁰ In the event that electronic coupling between the partners is sufficiently strong, k_{BC} is expected to correlate with the inverse of the solvent longitudinal reorientation time (τ_{L}).²¹ Although the choice of solvent is limited, and many solvents display complex dielectric relaxation behavior,²² it has been possible to collect kinetic data for **1** and **2** in a small series of different solvents at room temperature. It was observed that the nature of the solvent had no discernible effect on either k_{AB} or k_{BD} . This is to be expected since Förster-type energy transfer shows only a very weak dependence on solvent and the reorganization energy for TET is known to be small for these systems.⁸

In both nitrobenzene ($\tau_{\text{L}} = 5.0$ ps)²³ and benzonitrile ($\tau_{\text{L}} = 6.9$ ps),²⁴ where reorientation of the solvent is markedly slower than in acetonitrile ($\tau_{\text{L}} = 0.4$ ps),²⁵ the distal $^3\text{MLCT}$ state for **1** is not involved in the overall kinetic scheme, at least according to global analysis of the kinetic data under such conditions, and ILET is inhibited to such an extent that it hardly competes with TET to the $^3\pi,\pi^*$ state. For **2**, ILET still occurs but the rate is much slower than found in acetonitrile. Thus, k_{BC} values of 5.0 and $3.1 \times 10^{10} \text{ s}^{-1}$, respectively, were derived in nitrobenzene and benzonitrile. For **2** in butyronitrile ($\tau_{\text{L}} = 1.6$ ps),²⁵ k_{BC} was found to be $7.2 \times 10^{10} \text{ s}^{-1}$. The overall impression, therefore, is that the rate of ILET scales reasonably well with the inverse of the solvent reorientation time such that electron transfer must be fairly close to the adiabatic limit.

In summary, a strategy has been proposed that facilitates rapid population of the proximal $^3\text{MLCT}$ state. The significance of ILET can be visualized by monitoring buildup of the porphyrin-based $^3\pi,\pi^*$ state in conjunction with the model developed as Scheme 2. The rate constants derived for the various competitive steps give a detailed picture of the TET mechanism. Thus, ILET plays a minor role in dyad **1**, where the equilibrium constant ($K = 0.3$) lies on the side of the proximal $^3\text{MLCT}$ state. Population of the distal $^3\text{MLCT}$ state, following illumination with an ultra-short excitation pulse, is kept to a low level and its main contribution is to complicate the kinetics for formation of the $^3\pi,\pi^*$ state. In a solvent characterized by a particularly slow dielectric relaxation time, ILET is negligible for **1**. There is a modest thermodynamic driving force for ILET in dyad **2** and here the distal $^3\text{MLCT}$ state figures prominently in the TET process. The overall effect is to greatly decrease the rate of TET by directing the incident photonic energy away from the porphyrin acceptor. Such behavior, however, might be useful for directing energy transfer along predetermined pathways as an artificial neural network.

This work reports ILET on time scales of a few picoseconds, according to the thermodynamics of the system and the reorientation time of the solvent. We are unaware of any other report describing the dynamics of ILET in metal terpy complexes but estimates for the rate of ILET vary dramatically for

the corresponding 2,2'-bipyridine analogues. Thus, Hammarström et al.⁶ have found that ILET is complete within 1 ps for Ru(II) tris(2,2'-bipyridine) in acetonitrile at ambient temperature. This situation is consistent with their prior observation of very fast electron transfer in certain molecular dyads.⁷ In contrast, Mallone and Kelley^{3a} report that ILET occurs over about 50 ps under similar conditions and this value seems consistent with Meyer's estimate⁵ based on competitive energy transfer. Our approach has the advantage of dealing with a linear complex and with knowing which terpy ligand is excited via energy transfer. In our work carried out over many years with a variety of relevant dyads, we have not found energy transfer rates faster than ca. 10^{11} s^{-1} and this is in keeping with our estimated rate of ILET. A potential problem with our approach, however, is that formation of the proximal $^3\text{MLCT}$ state is fairly slow, especially for the Ru(II) complex, and this might obscure the kinetics for subsequent scrambling of the electron. The approach is also indirect and requires detailed analysis of energy-transfer rates.

Acknowledgment. We thank EPSRC (EP/D032946/1) and the University of Newcastle for financial support.

References and Notes

- (1) (a) Bradley, P. G.; Kress, N.; Hornberger, B. A.; Dallinger, R. F.; Woodruff, W. H. *J. Am. Chem. Soc.* **1981**, *103*, 7441–7446. (b) Mabrouk, P. A.; Wrighton, M. S. *Inorg. Chem.* **1986**, *25*, 526–531. (c) Braterman, P. S.; Harriman, A.; Heath, G. A.; Yellowlees, L. J. *J. Chem. Soc., Dalton Trans.* **1983**, 1801–1803.
- (2) (a) Cushing, J. P.; Butoi, C.; Kelley, D. F. *J. Phys. Chem. A* **1997**, *101*, 7222–7230. (b) Pogge, J. L.; Kelley, D. F. *Chem. Phys. Lett.* **1991**, *238*, 16–24. (c) Cooley, L. F.; Bergquist, P.; Kelley, D. F. *J. Am. Chem. Soc.* **1990**, *112*, 2612–2617. (d) Carroll, P. J.; Brus, L. E. *J. Am. Chem. Soc.* **1987**, *109*, 7613–7616. (e) Carlin, C. M.; DeArmond, M. K. *J. Am. Chem. Soc.* **1985**, *107*, 53–57. (f) Onfelt, B.; Lincoln, P.; Norden, B.; Baskin, J. S.; Zewail, A. H. *Proc. Natl. Acad. Sci. U.S.A.* **2000**, *97*, 5708–5713. (g) Liard, D. J.; Busby, M.; Farrell, I. R.; Matousek, P.; Towrie, M.; Vlcek, A., Jr. *J. Phys. Chem. A* **2004**, *108*, 556–567.
- (3) (a) Malone, R. A.; Kelley, D. F. *J. Chem. Phys.* **1991**, *95*, 8970–8976. (b) Yeh, A.; Shank, C.; McCusker, J. *Science* **2000**, *289*, 935–938.
- (4) Shaw, G. B.; Brown, C. L.; Papanikolas, J. M. *J. Phys. Chem. A* **2002**, *106*, 1483–1495.
- (5) Schoonover, J. R.; Dattelbaum, D. M.; Malko, A.; Klimov, V. I.; Meyer, T. J.; Styers-Barnett, D. J.; Gannon, E. Z.; Granger, J. C.; Aldridge, W. S.; Papanikolas, J. M. *J. Phys. Chem. A* **2005**, *109*, 2472–2475.
- (6) Lomoth, R.; Hapfl, T.; Johansson, O.; Hammarström, L. *Chem. Eur. J.* **2002**, *8*, 102–109.
- (7) Wallin, S.; Davidsson, J.; Modin, J.; Hammarström, L. *J. Phys. Chem. A* **2005**, *109*, 4697.
- (8) (a) Collin, J.-P.; Harriman, A.; Heitz, V.; Odobel, F.; Sauvage, J.-P. *J. Am. Chem. Soc.* **1994**, *116*, 5679–5690. (b) Flamigni, L.; Barigelletti, F.; Armaroli, N.; Ventura, B.; Collin, J.-P.; Sauvage, J.-P.; Williams, J. A. G. *Inorg. Chem.* **1999**, *38*, 661–667. (c) Flamigni, L.; Barigelletti, F.; Armaroli, N.; Ventura, B.; Collin, J.-P.; Sauvage, J.-P.; Williams, J. A. G. *Chem. Eur. J.* **1998**, *4*, 1744–1754. (d) Flamigni, L.; Armaroli, N.; Barigelletti, F.; Balzani, V.; Collin, J.-P.; Dalbavie, J.-O.; Heitz, V.; Sauvage, J.-P. *J. Phys. Chem. B* **1997**, *101*, 5936–5943. (e) Dixon, I. M.; Collin, J.-P. *J. Porphyrins Phthalocyanines* **2001**, *5*, 600–607. (f) Benniston, A. C.; Harriman, A.; Pariani, C.; Sams, C. A. *Phys. Chem. Chem. Phys.* **2006**, *8*, 2051–2057.
- (9) Benniston, A. C.; Chapman, G. M.; Harriman, A.; Mehrabi, M. *J. Phys. Chem. A* **2004**, *108*, 9026–9036. ACB
- (10) (a) Ziessel, R.; Hissler, M.; El-ghayoury, A.; Harriman, A. *Coord. Chem. Rev.* **1998**, *178*, 1251–1298. (b) Harriman, A.; Ziessel, R. *Coord. Chem. Rev.* **1998**, *171*, 331–339. (c) Harriman, A.; Ziessel, R. *Chem. Commun.* **1996**, 1707–1716.
- (11) (a) Mataga, N.; Taniguchi, S.; Chosrowjan, H.; Osuka, A.; Kurotobi, K. *Chem. Phys. Lett.* **2005**, *403*, 163–168. (b) Mataga, N.; Taniguchi, S.; Chosrowjan, H.; Osuka, A.; Yoshida, N. *Chem. Phys.* **2003**, *295*, 215–228. (c) Harriman, A.; Hissler, M.; Trompette, O.; Ziessel, R. *J. Am. Chem. Soc.* **1999**, *121*, 2516–2525.
- (12) Unlike the case with metal tetraphenylporphyrins, where the upper-excited singlet state has a lifetime of several picoseconds and fluoresces weakly, the S_2 lifetime for the FB unit employed herein is <1 ps.
- (13) (a) Hamilton, A. D.; Rubin, H.-D.; Bocarsley, A. B. *J. Am. Chem. Soc.* **1984**, *106*, 7255–7257. (b) Sessler, J. L.; Capuano, V. L.; Burrell, A.

K. *Inorg. Chim. Acta* **1993**, 204, 93–101. (c) Harriman, A.; Odobel, F.; Sauvage, J.-P. *J. Am. Chem. Soc.* **1994**, 116, 5481–5482. (d) Flamigni, L.; Marconi, G.; Dixon, I. M.; Collin, J.-P.; Sauvage, J.-P. *J. Phys. Chem. B* **2002**, 106, 6663–6671. (e) Dixon, I. M.; Collin, J.-P.; Sauvage, J.-P.; Flamigni, L. *Inorg. Chem.* **2001**, 40, 5507–5517.

(14) Benniston, A. C.; Harriman, A.; Li, P. Y.; Sams, C. A. *J. Phys. Chem. A* **2005**, 109, 2302–2309.

(15) The triplet energies of the osmium(II) bis-terpyridine units are readily obtained from low-temperature emission spectra while the energy of the triplet state localized on the porphyrin unit was obtained previously to be ca. 1.47 eV on the basis of phosphorescence spectra recorded at 77 K in the presence of excess iodoethane (see ref 6f).

(16) Grosshenny, V.; Harriman, A.; Ziessel, R. *Angew. Chem., Int. Ed. Engl.* **1995**, 34, 1100–1102.

(17) Unlike for electron-transfer processes in polar solvents, TET is usually accompanied by rather small reorganization energies since the geometry hardly changes. The value of 0.10 eV is taken from ref 6f.

(18) The driving force for ILET across the metal complex was derived from cyclic voltammetry studies made for the corresponding osmium(II) bis-terpyridine complexes in deoxygenated acetonitrile at $-20\text{ }^{\circ}\text{C}$. The effect of the ethyne substituent is considerably less than that found for the analogous ruthenium(II) bis-terpyridine complexes.

(19) Rips, I.; Jortner, J. *J. Chem. Phys.* **1987**, 87, 2090–2104.

(20) Hynes, J. T. *J. Phys. Chem.* **1986**, 90, 3701–3706.

(21) Sumi, H.; Marcus, R. A. *J. Chem. Phys.* **1986**, 84, 4894–4914.

(22) Weaver, M. J. *Chem. Rev.* **1992**, 92, 463–480.

(23) McManis, G. E.; Nielson, R. M.; Cochev, A.; Weaver, M. J. *J. Am. Chem. Soc.* **1989**, 93, 5533–5541.

(24) Grampp, G.; Landgraf, S.; Rasmussen, K. *J. Chem. Soc., Perkin Trans. 2* **1999**, 1987–1899.

(25) Kahlow, M. A.; Kang, T. J.; Barbara, P. F. *J. Phys. Chem.* **1987**, 91, 6452–6455.